Canadian Mineralogist
Vol. 28, pp. 757-769 (1990)

MICROSTRUCTURAL SIGNATURES AND GLIDE TWINS IN MICROCLINE, HEMLO, ONTARIO

JOSEPH C. WHITE
Centre for Deformation Studies in the Earth Sciences, Department of Geology, University of New Brunswick, Fredericton, New Brunswick E3B 5A3

ROBERT L. BARNETT
Department of Geology, University of Western Ontario, London, Ontario N6A 5B7

ABSTRACT

Transmission electron microscopy (TEM) has been used to examine microstructures in K-feldspar from a white K-feldspar, vanadian mica schist and a predominantly pink K-feldspar unit within the Hemlo, Ontario, gold deposit. Electron-microprobe analyses indicate only minor compositional differences between feldspars in the two units; the degree of Al–Si order is typical of low microcline for all samples. TEM identifies three dominant microstructural elements: twins, dislocations and voids. There is a progression from a heterogeneous, low-density twin texture in the larger grains to more homogeneous twinning, involving larger volumes of the crystals, in smaller matrix grains. Both twinned and untwinned regions are triclinic, with twinning occurring below the temperature of the $C2/m \rightleftharpoons C\bar{1}$ transformation. Untwinned grains have high densities of voids (fluid inclusions) and dislocations, whereas these features are uncommon in twinned feldspar. Collectively, the microstructures suggest formation of untwinned, void-rich triclinic grains from a feldspathizing fluid at a temperature below the monoclinic $\rightleftharpoons$ triclinic transition. These are subsequently deformed and twinned, with the formation of late-stage, defect-free untwinned grains. Generation and preservation of glide twins in the triclinic crystals require the initial creation of anti-ordered pseudotwins that are stabilized for time periods sufficient to allow diffusional reordering of Al and Si. If gold mineralization is linked to this event, ore formation must occur during a deformation event that postdated the peak of metamorphism.

Keywords: microcline, transmission electron microscopy, metasomatism, glide twins, Hemlo deposit, Ontario.

SOMMAIRE

Nous avons abordé l'étude des microstructures du feldspath potassique blanc dans un schiste à mica vanadifère et du feldspath potassique rose dans une unité feldspathique du gisement aurifère de Hemlo, en Ontario, par microscopie électronique par transmission. Les analyses à la microsonde électronique révèlent de faibles différences en composition entre les deux unités; le feldspath est un microcline ordonné dans tous les échantillons. Il y a trois éléments microstructuraux importants: macles, dislocations, et vacuoles. Il y a une faible densité de macles et une distribution hétérogène de celles-ci dans les grains les plus grossiers, tandis que dans les petits cristaux de la matrice, la répartition des macles est plus homogène, et ces macles occupent un volume plus important des cristaux. Les domaines maclés et non maclés sont tous tricliniques; les macles ont pris naissance à une température inférieure à celle de la transition $C2/m \rightleftharpoons C\bar{1}$. Les cristaux non maclés possèdent une forte densité de vacuoles (inclusions fluides) et de dislocations, tandis qu'elles ne sont pas fréquentes dans le microcline maclé. D'après l'ensemble des microstructures, il y aurait eu formation d'un feldspath triclinique non maclé et riche en vacuoles à partir d'une phase fluide "feldspathisante", à une température inférieure à celle de la transition monoclinique $\rightleftharpoons$ triclinique. Ces grains ont par la suite été déformés et maclés; la formation d'un microcline sans dislocation est venue tardivement. La génération et la préservation de macles impliquant un glissement dans les cristaux tricliniques supposent la création de pseudo-macles anti-ordonnées qui sont stabilisées pour une période de temps suffisante pour permettre la mise en ordre des cations Al et Si par diffusion. Si la minéralisation en or est liée à cet événement de déformation, le minerai doit être postérieur au paroxysme métamorphique et cinématique.

(Traduit par la Rédaction)

Mots-clés: microcline, microscopie électronique par transmission, macles de glissement, gisement de Hemlo, Ontario.

INTRODUCTION

Previous investigations of the Hemlo, Ontario, gold deposit and associated rocks have addressed the stratigraphic and structural relationships of the area, the geochemistry of the rocks and mineral chemistry (Muir 1983, 1986, Hugon 1984, 1986, Cameron & Hattori 1985, Harris 1986, Valliant & Bradbrook 1986, Walford *et al.* 1986). In this contribution, we describe textures observed by transmission electron microscopy (TEM) from K-feldspar-rich units within the ore zone. These rocks are of critical importance to any model of ore generation because they reflect potassium enrichment centered on the ore zone. Although the latter spatial association has been reported throughout the Hemlo camp, there is neither general agreement as to the timing and origin of the altering fluids (Muir 1986), nor a uniquely established temporal relationship between Au mineralization and K metasomatism. Whereas some authors have linked K-feldspathization with events of synmetamorphic to late metamorphic deformation (Hugon 1986, Walford *et al.* 1986), others have explicitly favored pre- or early metamorphic hydrothermal fluids for the alteration (Kuhns *et al.* 1986, Valliant & Bradbrook 1986).

The feldspathic units are spatially associated with each other and the ore zone (Walford *et al.* 1986), but outwardly suggest distinct metamorphic or metasomatic histories: unit M1 is a schist that contains white to grey K-feldspar, quartz, and vanadian muscovite; unit M2 comprises bright pink to red K-feldspar. It was conjectured that electron-diffraction contrast might image intracrystalline features indicative of contrasting histories. In particular, the occurrence of abundant tapering twins, a morphology associated with mechanical twinning, suggested an interesting deformational aspect to the microstructure. The latter is of particular interest given the absence of unambiguous mechanical twins in K-feldspar (Smith & Brown 1988). The investigation is otherwise justified by the paucity of TEM information on K-feldspar in ore-forming environments.

Geological Setting

The Hemlo deposit is situated approximately 35 km east of Marathon, Ontario, along the Trans-Canada Highway (Fig. 1). The regional setting of the deposit within a Late Archean greenstone belt has been summarized by Muir (1983). Samples were taken from drill core collected at the Page–Williams property, for which detailed descriptions of the geology have been given by Walford *et al.* (1986). Major lithologic units strike 108° and dip 60–70° NE, and all Au mineralization is hosted by rocks with secondary microcline (Walford *et al.* 1986). The ore zone has been reported to occur at the contact between hanging-wall metasedimentary and footwall volcanic rocks (Valliant & Bradbrook 1986), although lithologic and structural complexities preclude a simple relationship (Muir & Elliott 1987). The metasedimentary rock units structurally above the ore zone have abundant amphibolite-grade minerals, including kyanite, staurolite and garnet (Walford *et al.* 1986). Amphibole and garnet in disequilibrium with the latter assemblage are recognized within the uppermost sections of the ore zone. Burk *et al.* (1986) described two metamorphic events at the adjacent Teck–Corona deposit, with a high pressure (700 MPa) event preceding metamorphism at about 500 MPa.

Regional deformation within a zone of ductile shear 5–10 km wide has been postulated to have occurred at conditions of peak metamorphism (Hugon 1986), with pervasively intense deformation centered on the ore deposit (Muir 1986). A detailed structural study by Muir & Elliott (1987) identified four generations of deformation. Major D_2 folds define the regional structure and predate the peak metamorphism; displacements during this event were sinistral. D_3 folding and penetrative dextral shear affected the area during and after growth of garnet and staurolite porphyroblasts. Synthesis of these data led Muir & Elliott (1987) to argue for an oblique, transcurrent dextral shear, as opposed to the predominantly progressive, oblique southeasterly thrusting suggested by Hugon (1986).

Muir & Elliott (1987) also explicitly demonstrated

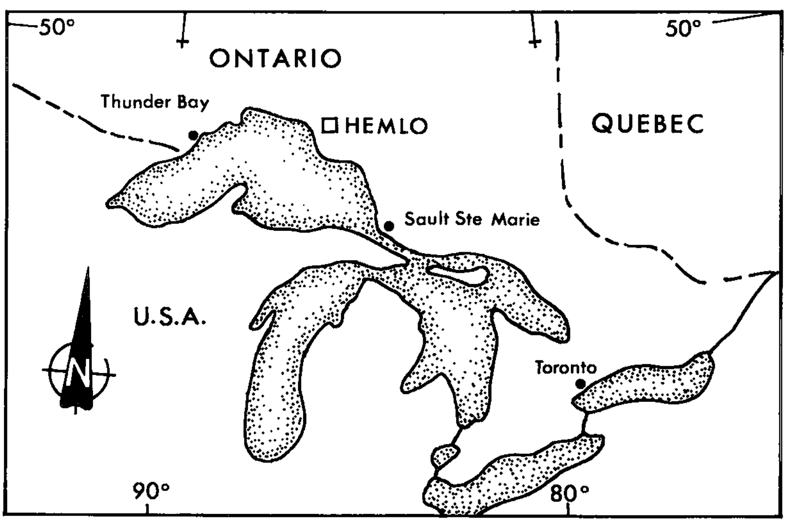

FIG. 1. Location map for the study area.

that the main Hemlo orebody is parallel to the L_2 lineation, in correspondence with the observations by Walford *et al.* (1986) that the "early" folds, which have a foliation parallel to the regional lithological trend, plunge parallel to the Main Ore Zone. Burk *et al.* (1986) placed development of high-strain zones on the Teck–Corona site within their lower-pressure event, after "early" folding, with contemporaneous Au–Mo mineralization and K-metasomatism.

Experimental Techniques

Standard petrographic thin sections of each unit were examined, with concentration on those areas that seemed to consist of optically monomineralic K-feldspar. Mineral compositions were determined by wavelength-dispersion analysis with a JEOL 733 electron microprobe operated at 15 kV, 10 nA current and a beam diameter of 10 μm. Powder-diffraction data were collected with an automated Philips 1050/81 X-ray diffractometer; three powder samples were examined from each lithologic unit. Cell refinements followed the method of Appleman & Evans (1973) and are based on a minimum of 29 reflections. The degree of Al–Si order characteristic of the feldspar in each lithologic unit was calculated from the equations given by Kroll & Ribbe (1987). Areas for TEM analysis were identified in thin section, mounted on copper grids and ion-thinned to perforation. Most TEM examinations were carried out with a Philips EM400T operated at 120 kV. Additional observations and compositional analyses were made using an EM400T with energy dispersion X-ray analysis capabilities, operated at 100 kV.

Sample Description

Unit M1

Consistent with its appearance in hand specimen as a massive white microcline rock, petrographic thin sections of M1 contain predominantly K-feldspar. Quartz occurs as fine veins and disseminated matrix grains, with grains of albite, titanite, chlorite, calcite and Fe-oxide forming minor and heterogeneously distributed components of the rock. The foliation is defined by green vanadian muscovite and pyrite. A characteristic mode is: 84% K-feldspar, 6% quartz, 6% pyrite, 3% muscovite, plus the remaining minor phases. Results of electron-microprobe analyses of K-feldspar M1 are listed in Table 1. Whereas Ba-rich K-feldspar with up to 16.6 wt.% BaO has been reported from the ore zone (Harris 1986), the grains studied here have an average content of only 0.57 wt.% BaO. Analytical TEM showed all microcline to be pure K-feldspar, with Na restricted to rare albite exsolution lamellae that are concentrated in the larger grains. The Na_2O content

TABLE 1. ELECTRON-MICROPROBE DATA ON THE K-FELDSPAR IN M1 AND M2

	M1-11	M1-12	M1-13	M1-14	M1-15	M1-16	M1-17	M1-AVG
SiO_2	64.41	64.95	64.47	65.29	64.45	63.53	63.85	64.42
TiO_2	0.04	0.02	0.02	0.04	0.00	0.04	0.03	0.03
Al_2O_3	18.22	17.96	18.13	18.21	17.95	18.15	18.21	18.12
FeO	0.00	0.07	0.07	0.09	0.08	0.11	0.08	0.07
MnO	0.00	0.00	0.00	0.00	0.02	0.00	0.00	0.00
CaO	0.00	0.00	0.00	0.00	0.00	0.00	0.00	0.00
MgO	0.00	0.00	0.00	0.00	0.00	0.00	0.01	0.00
Na_2O	0.40	0.34	0.33	0.40	0.38	0.44	0.35	0.38
K_2O	15.88	16.05	15.92	15.97	16.02	16.23	16.29	16.05
BaO	0.56	0.54	0.59	0.56	0.58	0.50	0.65	0.57
TOTAL	99.51	99.93	99.53	100.56	99.48	99.00	99.47	99.64
	M2-4	M2-5	M2-6	M2-7	M2-8	M2-9	M2-10	M2-AVG
SiO_2	65.58	64.80	65.28	65.02	65.24	65.21	65.12	65.17
TiO_2	0.01	0.00	0.04	0.00	0.05	0.00	0.00	0.01
Al_2O_3	18.36	17.79	17.83	18.10	18.10	18.08	18.02	18.04
FeO	0.06	0.08	0.08	0.06	0.05	0.07	0.00	0.06
MnO	0.00	0.00	0.00	0.00	0.02	0.01	0.02	0.01
CaO	0.00	0.00	0.06	0.00	0.00	0.00	0.00	0.01
MgO	0.00	0.00	0.00	0.00	0.00	0.00	0.00	0.00
Na_2O	0.21	0.38	0.22	0.30	0.41	0.36	0.25	0.30
K_2O	16.48	16.36	16.49	16.44	16.02	16.37	16.40	16.37
BaO	0.16	0.24	0.23	0.17	0.17	0.16	0.19	0.19
TOTAL	100.86	99.65	100.23	100.09	100.06	100.26	100.00	100.15

Concentrations expressed in wt.%. Operating conditions described in Experimental Techniques in text.

TABLE 2. CELL PARAMETERS AND Al OCCUPANCY OF THE T_1 POSITION

	a Å	b Å	c Å	α	β	γ	t_1O+t_1m
M1	8.561(2)	12.968(5)	7.217(4)	90.62°	115.84°	87.68°	0.99
M2	8.562(2)	12.964(1)	7.215(3)	90.62°	115.86°	87.68°	1.01

identified by microprobe analysis either is too small to be recorded by EDS in the TEM or else the microprobe is sampling albite lamellae that can be avoided in the TEM. The cell parameters of the K-feldspar are given in Table 2. The feldspar is low microcline with $t_1O + t_1m = 0.99$.

Because non-feldspar phases commonly are concentrated within narrow foliation bands or discrete veins, large areas of a given thin section are effectively monomineralic microcline. Although microstructures even in these monomineralic regions can vary widely and abruptly, a few principal elements can be recognized. The grain size of the microcline ranges between 20 and 500 μm; grains generally have an equant shape (Fig. 2a). Large grains are contained within a matrix of smaller recrystallized grains. Within mica-rich bands, microcline single crystals 500 μm long, with an aspect ratio of 4:1, are observed. Fluid and mineral inclusions occur throughout the microcline grains, but are particularly evident in the larger grains. The inclusions are dispersed throughout the grains (Figs. 2b, c) and display only an occasional association with recognizable healed fractures. Matrix grains exhibit both equilibrated polygonal textures and irregular grain boundaries. Undulose extinction, characteristic of subgrain development, is particularly well developed in the matrix grains (Fig. 2a). The combination of

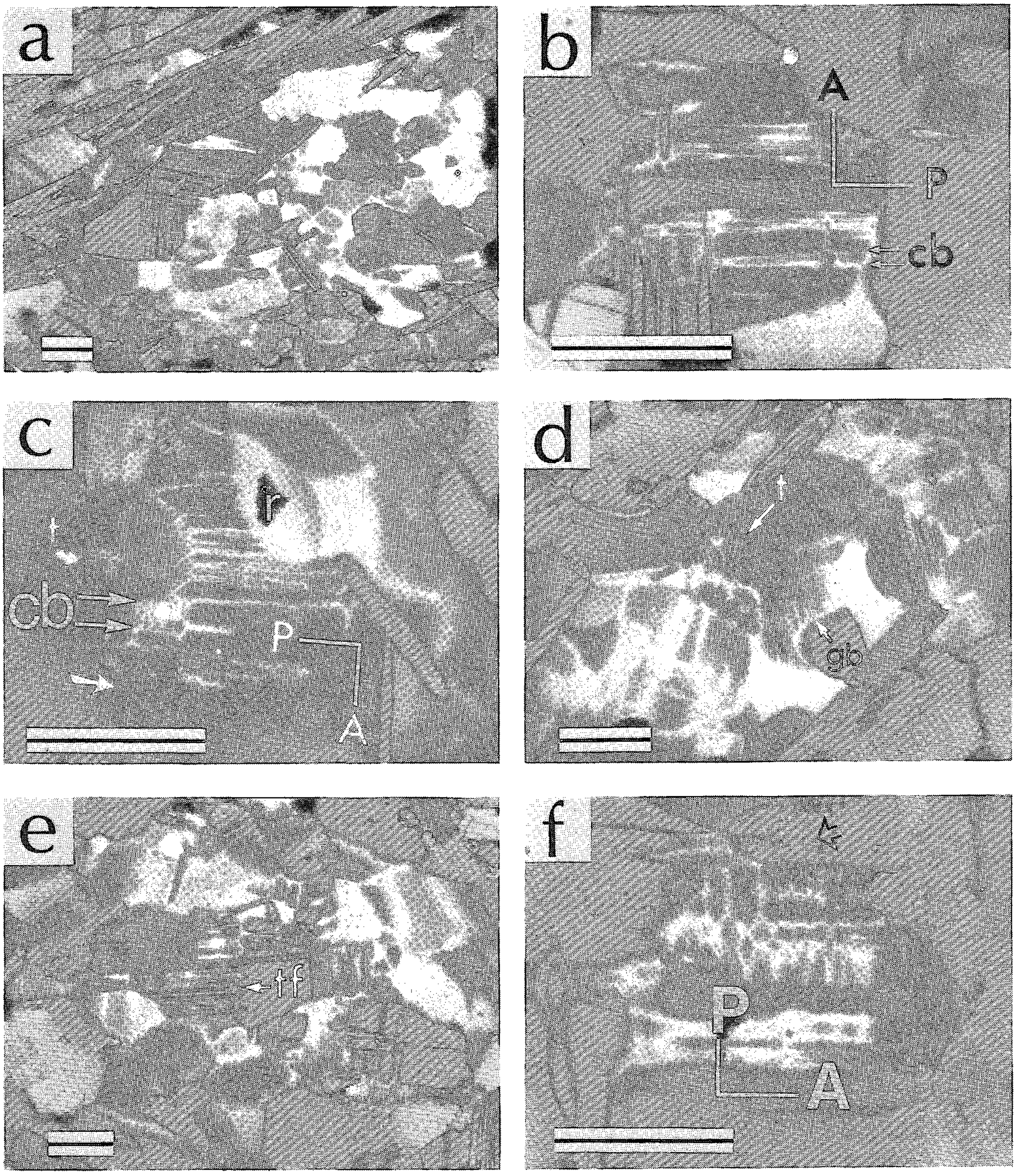

FIG. 2. Optical micrographs of Hemlo feldspars. Scale bars: 100 μm. a) Overview of M1 microstructures. Foliation is defined by mica. Large twinned grain is surrounded by finer-grained matrix. b) Grain with contrast typical of Albite (A) and Pericline (P) twins. Contrast bands (cb) consist of fine lamellar contrast features parallel to A-twins that are aligned in bands parallel to P-twin orientations. c) M1 grain with A- and P-twins with contrast bands (cb) and terminating A-twins (t). Inclusions (arrowed) are abundant in untwinned regions. Untwinned, recrystallized grains (r) postdate larger twinned grain. d) Terminating twins (t) initiate at grain boundaries (gb) in M1. e) Irregular twin front (tf) in M2. f) Discrete A-twins and lozenge-shaped domains parallel P-twin orientation comprising fine A-twins. Inclusions are indicated by the arrow.

optical deformation features and polygonal grains strongly suggests grain-size reduction during dynamic recrystallization. Recrystallization can also be recognized as inclusion-free, untwinned, lensoid grains that postdate the larger, twinned, inclusion-rich microcline (Fig. 2c).

As previously noted by Harris (1986), twins are common in the microcline, but not ubiquitous. Grains commonly show no optical twins, and even grains with twins can have large volumes of un-

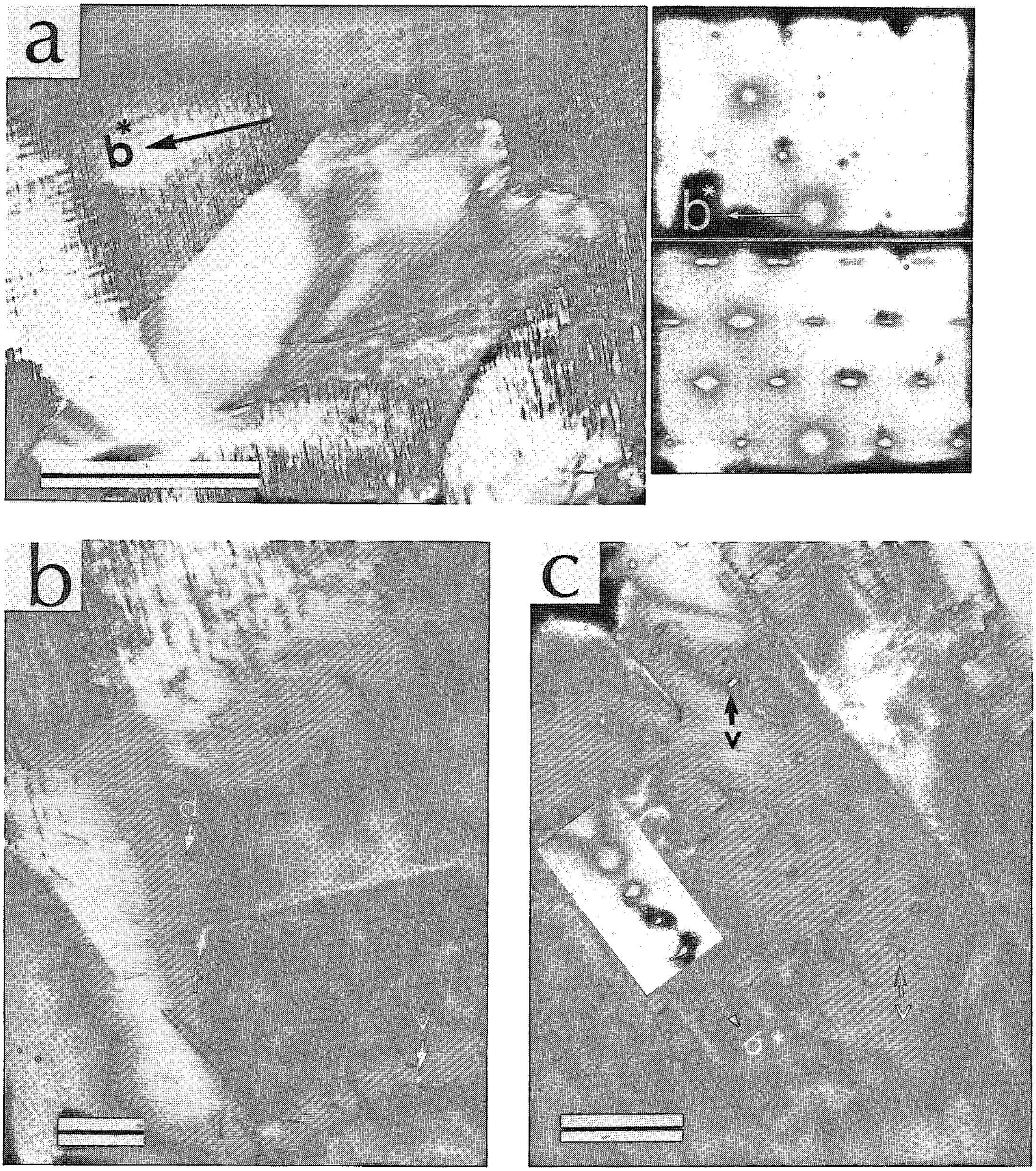

FIG. 3. TEM micrographs of M1 K-feldspar. Scale bars: 1 μm. a) K-feldspar grain surrounded by A-twinned feldspar of the same composition. Electron-diffraction patterns with **B** = [001] show the triclinic nature of untwinned (upper) and twinned (lower) grains. b) Transitional twin front between domains. Dislocations (d) and voids (v) are concentrated in the untwinned domain. A microfracture (f) also is evident. c) Large grain with dispersed P-twins that are partially transformed to A-twins. The grain contains abundant dislocations and voids (v). **B** = [104].

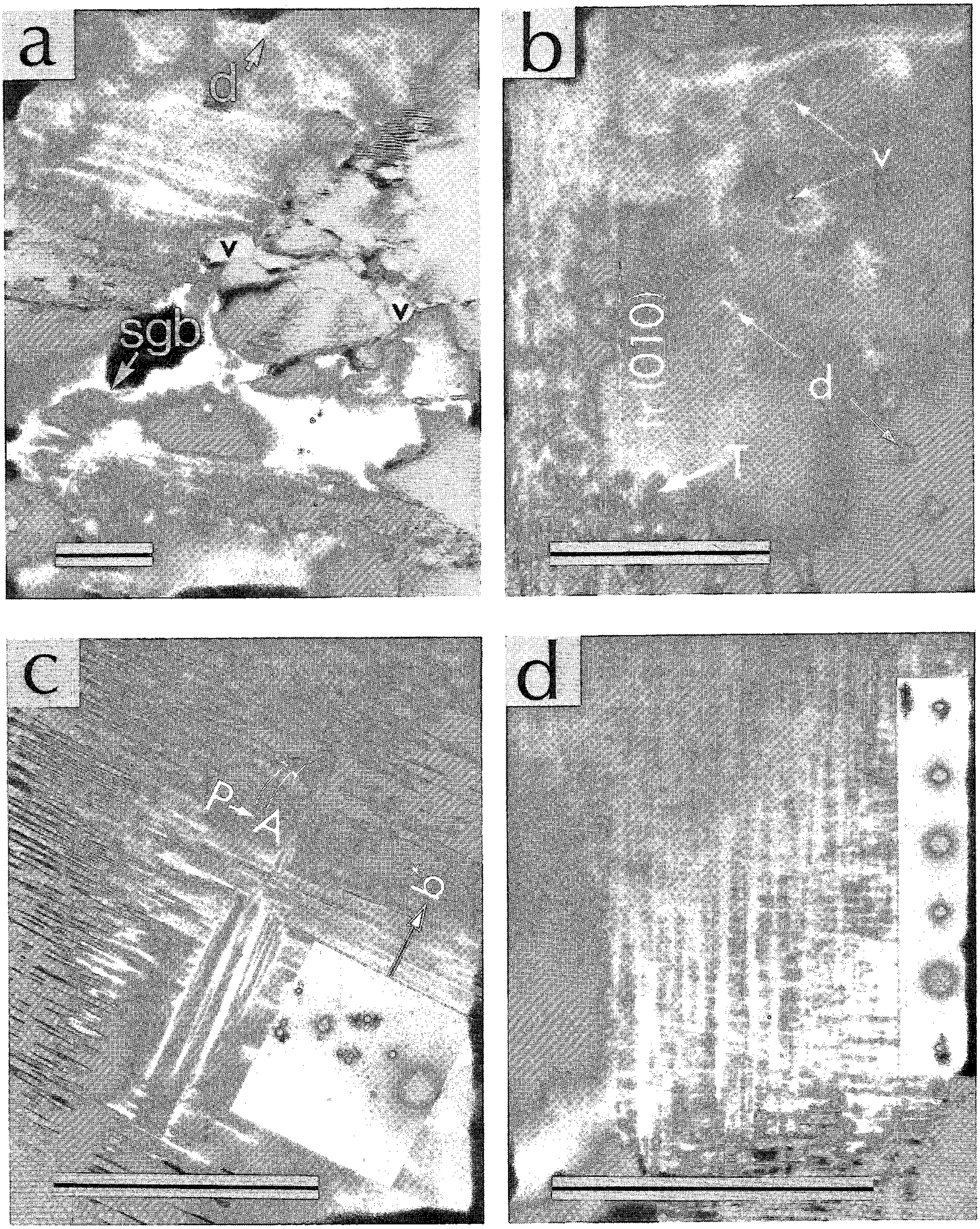

FIG. 4. TEM microstructures in M2 K-feldspar. a) Islets of Albite-twinned feldspar in a matrix of deformed untwinned microcline containing abundant subgrain walls (sgb) and dislocations (d). Voids (v) are concentrated along subgrain boundaries. Scale bar: 1 μm. b) Twin front with Albite twins (T) inclined to beam, as indicated by fringes. Voids (v) and dislocations (d) are concentrated in the untwinned feldspar. **B** = [112]. Scale bar: 1 μm. c) Mixed A- and P-twins. P-twins are in the process of transforming to fine Albite twins. **B** = [001]. Scale bar: 1 μm. d) Tartan-like texture in Albite twin domain. The modulation developed parallel to the (0*k*0) reflections has no corresponding effect on the diffraction pattern except for minor streaking. **B** = [104]. Scale bar: 500 nm.

twinned feldspar. Both Pericline law (P) and Albite law (A) twins are observed, but rarely do they form the classic cross-hatched twin textures. Whereas in some grains, discrete P- and A-twins can be identified (Fig. 2b), other grains exhibit fine A-twins developed along contrast bands parallel to the expected P-twin orientation (Figs. 2b, c). Sharp, wedge-shaped, terminating twins typical of mechanical twins (Starkey & Brown 1964, Vernon 1965, Brown & Macaudière 1986) are abundant (Figs. 2c, d). These tapering twins commonly originate at grain boundaries and triple junctions, and their terminations are usually associated with other microstructures, including twins of the other twin law, optical subgrain boundaries, grain boundaries and inclusions.

Quartz occurs as both single crystals up to 1 mm in diameter, elongate parallel to the foliation, and small dispersed grains (20–100 μm). Deformation lamellae and subgrains are observed, and healed cracks are clearly identified by trails of inclusions. Strongly deformed quartz–calcite aggregates contain fiber growths characteristic of veins or some comparable solution–precipitation origin. Micas form a C–S-type two-foliation deformation texture (Berthé *et al.* 1979).

Unit M2

The combination of bright pink to red feldspar and irregular patches of calcite and chlorite, with minor titanite, gives unit M2 a more altered, less pristine appearance in hand specimen than M1. Modal analyses are typically 90 - 95% K-feldspar. Feldspar compositions and cell parameters are listed in Tables 1 and 2, respectively. The feldspar in M2 has markedly less Ba than in M1, but otherwise is similar. As in M1, the K-feldspar is low microcline, with $t_1O + t_1m = 1.01$.

The grain-size variation is the same as in M1 with, again, a general absence of equilibrium grain boundary textures. Optically observed twins are common, but are generally less well defined than in M1. Transgranular twins are anastomosing (Fig. 2e), with some fine, patchy twin domains giving an initial impression of sericitization. Terminating A-twins aligned within bands parallel to the P-twin orientation are very common. Such bands can be lozenge-shaped with intragranular terminations (Fig. 2f). Inclusions in grains are very common. The density of inclusions is sufficiently high in some areas to give an altered appearance. Deformation-induced undulose extinction, reflecting the occurrence of subgrains, occurs throughout the specimen. The foliation is less pronounced than in M1 because of the absence of a dominant phyllosilicate phase and is instead defined by bands of varying grain-size. Quartz features are as described for M1.

Transmission Electron Microscopy

The microstructures in both M1 and M2 lithologies consist of three dominant elements: twins, voids and dislocations. These combine to create an overall texture of intimately associated twinned and untwinned regions in the microcline. No compositional difference between these regions can be identified with the TEM. Both dislocations and voids are concentrated in untwinned material, with slightly different textures in M1 and M2.

Juxtaposed twinned and untwinned microcline produce a distinctly heterogeneous microstructure. Untwinned microcline occurs as discrete grains surrounded by twinned material (Fig. 3a) and intragranular domains having diffuse boundaries with twinned regions of the same crystal (Fig. 3b), whereas large, predominantly untwinned grains contain isolated, dispersed twins (Fig. 3c). Selected-area diffraction has identified only triclinic symmetry in both twinned and untwinned regions (Fig. 3a), in agreement with the X-ray-diffraction data. Twin microstructures in large grains and the finer matrix are distinctly different. Large grains have a heterogeneous, low-density twin texture with long P-twins exhibiting the well-established degeneration (*e.g.*, Fitz Gerald & McLaren 1982) to bands of fine A-twins (Fig. 3c). As grains become more completely twinned, as is characteristic of the small matrix grains, A-twins dominate (Fig. 3a) and form the most homogeneous twin texture observed. The interaction of the dominant A-twins with P-twins forms a host of window textures of the types reviewed by McLaren (1984), whereas the systematic termination of A-twins, presumably along a degenerate P-twin composition plane, continues to create bands of contrast nearly perpendicular to the (010) twin planes.

In addition to the textures observed in M1, twinned microcline islets are commonly surrounded by untwinned microcline in M2 (Fig. 4a). Figures 4a and 4b show the irregular intercrystalline and transitional intracrystalline nature of many of the twin fronts and the concentration of voids and dislocations in the untwinned material. A-twins again predominate, with the commonly observed transformation of P-twins to fine A-twins. As in M1, the juxtaposition and intersection of A- and P-twins and systematic termination of A-twins along degenerate P-twin boundaries produce contrast-band and window textures (Fig. 4c), which have been reviewed by McLaren (1984). Strong tartan patterns produced by fine A- and P-twins are common, particularly in islet grains (Fig. 4d).

The transition from untwinned to twinned microcline is recorded by intracrystalline twin-domain boundaries. The majority of these form as broad transition zones from contrast-free untwinned

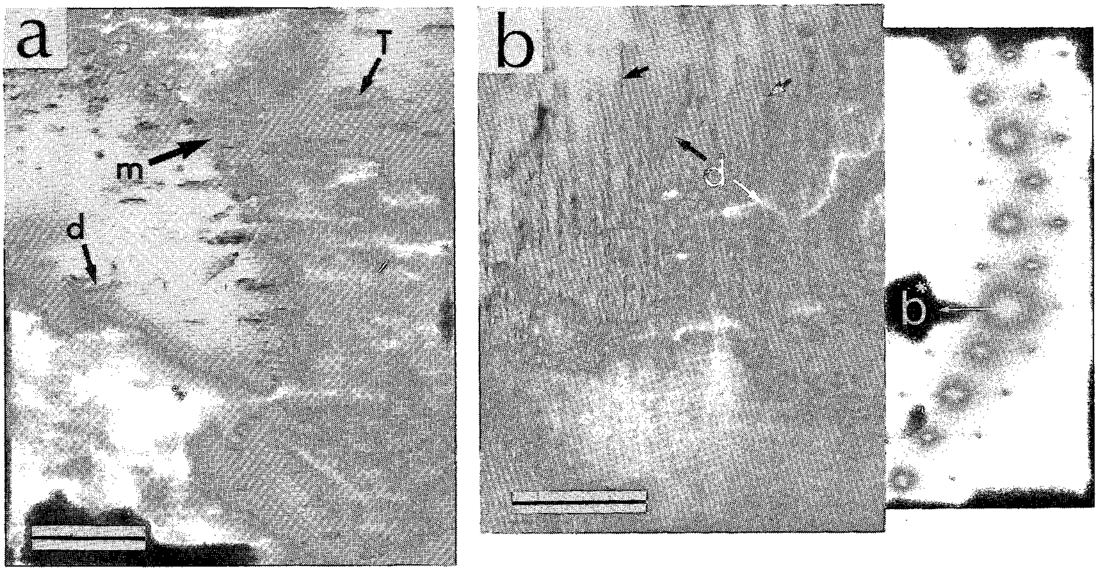

FIG. 5. Twin fronts. Scale bars: 1 μm. a) Isolated Albite-law microtwins (T) and dislocations (d) in transition zone between domains. A modulated or tweed texture (m) is imaged where the deviation parameter s is locally perturbed along a bend contour. b) Transitional zone between twinnned domain (bottom) and untwinned microcline (top) in M1 with dislocations (d). The diffraction pattern shows extensive distortion in terms of streaking of (0k0) reflections, caused by the high density of defects (arrowed), at least some of which are dislocations, but no discrete twin reflections. $\mathbf{B} = [001]$.

to twinned microcline, with progressively higher densities of microtwins (Figs. 4b, 5a). However, some domain boundaries are particularly diffuse (Fig. 5b), with twin-parallel crystal defects causing streaking of primary reflections in selected-area electron-diffraction patterns. An apparent tweed texture, that is usually associated with intermediate states of Al–Si order, *i.e.,* between low microcline and orthoclase, and is a precursor to transformation twinning, has been observed in proximity of this twinning front (Fig. 5a). Attempts to enhance the tweed-texture contrast throughout the samples by varying the diffraction error s (McLaren & Fitz Gerald 1987) did not increase the frequency of observation.

Abundant voids and dislocations occur within the untwinned microcline of both lithologic units, whereas there is a near-mutual exclusion of voids and dislocations from homogeneously twinned domains (Figs. 3, 4). An exception to the latter are untwinned, lensoid grains (Fig. 3a), similar to some recrystallized grains observed by light microscopy (Fig. 2c), that contain neither voids nor dislocations. The combination of a regular shape and the absence of crack-healing-related defect contrast suggests that the voids had a primary origin during crystal growth. Dislocations are abundant in the untwinned microcline up to the twin domain interfaces (Figs. 3b, 4b), but are only rarely observed in the twinned feldspar (Fig. 6a) despite the use of a wide range of imaging conditions.

Comparison of trace analysis data, line directions and limited invisibility-contrast experiments with known slip systems (Gandais & Willaime 1984) allow some inferences to be made as to the dislocation glide systems. In M1 grains, these data suggest $\mathbf{B} = 1/2<112>(20\bar{1})$ as a slip system, whereas other dislocations in twinned microcline at the twin front (Fig. 6a) have segments perpendicular to possible $<110>$ and $<101>$ slip directions. Dislocation networks are particularly well developed in the recrystallized matrix of M1. Dislocation orientations in the networks are commonly related to rational crystallographic slip planes. In Figure 6b, subgrain boundaries are parallel to $(1\bar{1}0)$ and (101) traces, whereas other networks show dislocation segments that lie parallel to or near (010), (001), $(\bar{1}11)$ and $(11\bar{1})$ traces. The latter has segments that are perpendicular to possible $<110>$ type slip directions.

In general, dislocation densities are lower in M2 than in M1, with many untwinned regions containing only a few dislocations, commonly as components of a network. End-on dislocation contrast was observed for the electron beam parallel to [112] and [110], which, by comparison with known glide systems, is consistent with screw dislocations lying parallel to these directions. Despite the lower concentration of free dislocations, the abundance of subgrain structures indicates the contribution of deformation to the overall texture.

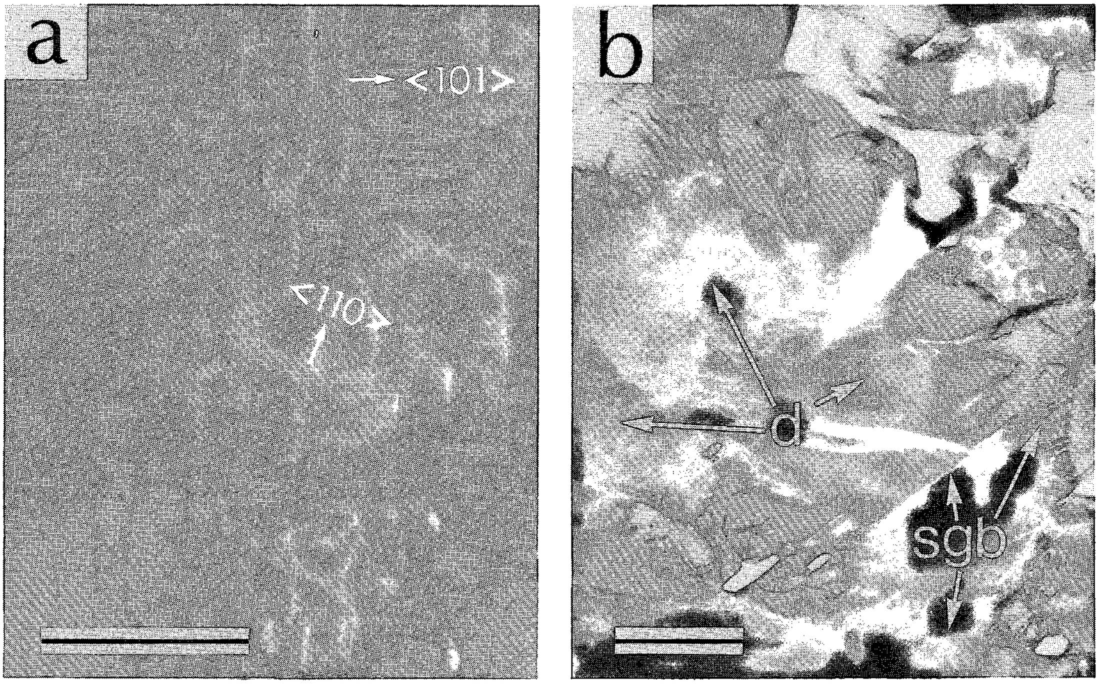

FIG. 6. Defect microstructures. Scale bars: 1 μm. a) Dislocations at twin front imaged near (111) with bowed segments perpendicular to expected slip directions <101> and <110>. b) Deformation substructure resulting from dislocation walls defining subgrain boundaries (sgb), which in turn contain free dislocations (d). Subgrain boundaries are parallel to traces of $(1\bar{1}0)$ and (101).

DISCUSSION

Igneous and metamorphic rocks have provided the source material for most TEM studies of K-feldspar (McLaren 1984, Smith & Brown 1988). Exceptions include Smith & McLaren (1983), who examined a presumed metasomatic microcline from Greenland, and Guthrie & Veblen (1988) who described alkali feldspar from hydrothermally altered granites. Likewise, microstructures in the Hemlo microcline are considered to reflect a metasomatic origin. In turn, these microstructures provide circumstantial evidence for the conditions and timing of metasomatism, in addition to and independent of the bulk chemistry of the rocks and the relevant field observations.

The existence of untwinned microcline grains and domains, in conjunction with the degree of Al–Si ordering inferred by X-ray diffraction, argues for direct formation of the microcline as a triclinic phase below the temperature of the monoclinic ⇌ triclinic transformation. This conclusion is supported by reference to the absence of twinning in authigenic triclinic K-feldspar, which has been presented as evidence for a primary triclinic origin (Finney & Bailey 1964, Kastner & Siever 1979). A tendency for authigenic feldspars formed between 0 and 300° C to have end-member compositions (Kastner & Siever 1979) also is similar to the observed purity of the Hemlo microcline studied. Voids in the untwinned microcline are interpreted as having been fluid inclusions that were incorporated during formation of the grains by a potassium-rich fluid. Similar features have been reported by Guthrie & Veblen (1988) in clouded alkali feldspar. The absence of associated healed fractures in TEM favors this primary origin for the voids during crystal growth. Metasomatism thus provides a mechanism for the formation of primary microcline, introduction of the high density of voids (fluid inclusions) into these grains and fluid-assisted Al–Si ordering at low temperature.

An origin of the Hemlo K-feldspar as primary microcline would require that the temperature of the metasomatic fluid be less than that for the monoclinic ⇌ triclinic transformation. The upper stability of low microcline is placed by Brown & Parsons (1989) at about 450° C, which in turn is less than the peak metamorphic temperatures at mid-amphibolite grade reported at Hemlo. The abundant dislocations and substructures are evidence that significant deformation occurred after formation of the untwinned microcline; however, neither the free dislocations nor the voids could be expected to survive amphibolite-facies deformation, recovery and recrystallization in a rate-enhancing, fluid-saturated environment. The preservation of these features is further evidence that the relevant metasomatism and subsequent deformation occurred during cooling after the peak of metamorphism, rather than at a pre- or synmetamorphic stage.

Twinning of the void-bearing microcline at Hemlo must postdate its formation from metasomatic fluids. This is particularly evident at intracrystalline twin fronts, where isolated microtwins are developed within an untwinned, triclinic host. In conflict with this observation is the demonstrated association of microcline twinning with Al–Si ordering and the resultant inversion from monoclinic to triclinic symmetry (McLaren 1984, Smith & Brown 1988, Brown & Parsons 1989). The ubiquity of polysynthetic twins in microcline that has initially crystallized at temperatures above the symmetry transition makes such twins a virtual characteristic of microcline (*e.g.*, McLaren 1978). However, it has been noted by Smith & McLaren (1983), amongst others, that microcline twins need not be *intrinsically* associated with the symmetry break. The evidence pointing to a low-temperature origin for the Hemlo microcline requires an alternative to transformation twinning.

Many twins in the Hemlo microcline are morphologically similar to mechanical twins described in plagioclase (Vance 1961, Starkey & Brown 1964, Vernon 1965, Brown & Macaudière 1986); for example, lenticular twins that initiate at grain boundaries, taper and terminate within grains. True glide twins have been precluded from ordered triclinic plagioclase because of the resultant anti-ordered distribution of Al–Si in the twin (Laves 1952, Starkey 1967) that does not reproduce the crystal structure. However, the formation of these anti-ordered *pseudotwins* remains mechanically plausible, albeit with an expected tendency to untwin upon relaxation of the external stress due to the inherent instability arising from the Al–Si site distribution (*e.g.*, Marshall & McLaren 1977).

The rejection of undoubted mechanical twins in plagioclase on crystallographic grounds has been addressed (Brown & Macaudière 1986, Brown 1989a, b) by defining the conditions necessary for and the viability of nucleation and preservation of glide twins or pseudotwins. Interim stabilization of pseudotwins during diffusional reversal of the Al–Si site occupancy to convert pseudotwins to twins requires either the maintenance of an imposed stress to prevent untwinning or internal relaxation of the untwinning stresses (Brown & Macaudière 1986). The latter can be achieved through interaction with and termination against interfaces, such as other twins and grain boundaries, which removes residual stresses in the crystal.

Mechanical twinning in microcline has been similarly precluded on the basis of the inability of glide twinning to reproduce the ordered crystal structure (*e.g.*, Tullis 1983). However, Smith & Brown (1988, p.553) noted that there is no reason why pseudotwins could not form in microcline, analogous to those in plagioclase. In microcline of igneous or metamorphic origin, there is a fundamental difficulty in differentiating between transformation and purely mechanical twins, particularly if the morphologies are not distinctive (Brown & Macaudière 1986) and where deformation is often essential to the process of transformation twinning (Eggleton & Buseck 1980). Similarly, authigenic microcline could be expected to remain untwinned, if for no other reason than it is characteristically identified in environments in which deformation is absent. We suggest that the environment at Hemlo provided conditions for both the development and preservation of glide twins. These conditions were: 1) formation of a primary, untwinned triclinic feldspar, 2) subsequent deformation of these crystals, which generated pseudotwins (by necessity), 3) stabilization of these pseudotwins by the defect microstructure, either permanently or long enough to enable, 4) fluid-enhanced redistribution of Al and Si in the anti-ordered (pseudotwinned) domains to produce an ordered (twinned) structure.

Essential to this process is the metasomatism of the Hemlo rocks, both for the formation of primary microcline and for the enhancement of Al–Si rates of diffusion that would be expected in a fluid-rich environment. The driving force for untwinning should decrease as the difference in order between ordered and anti-ordered regions is reduced (Brown & Macaudière 1986), thus making an efficient redistribution of Al and Si efficacious to the preservation of the glide twins.

In the Hemlo microcline, twin terminations were commonly observed in the petrographic microscope to be associated with high concentrations of fluid inclusions. Similarly, TEM observations emphasized the contrast between twinned and untwinned microcline, with the virtual absence of dislocations and voids in the twinned material except within transitional, intracrystalline twin fronts. The strain energy introduced to the crystal by these defects can be viewed as contributing to both the propagation and stabilization of the twins.

Dislocations are direct evidence that the external stress causes deformation of the microcline crystals, whereas the relatively high density of dislocations within untwinned microcline indicates that glide twinning is not an "easy" deformation mechanism, as is expected for energetically unfavorable pseudotwins (Brown 1989a). The irregular and transitional twin interfaces can then be considered analogous to a recrystallization front. The distortion in untwinned microcline introduced by dislocations and voids provides a driving force for continued propagation of twins into volumes of untwinned crystal, while at the same time providing a mechanism for the inhibition of untwinning through the accommodation by these defects of elastic strains at the pseudotwin terminations. Absorbtion of defects and enhanced diffusion at the twin front, aided by the high activity of fluid, lead to effective sweeping-out of these defects from the crystal as the twin front passes, again in analogy to recrystallization (Urai *et al.* 1986).

Are there alternative interpretations to that of primary metasomatic microcline that is subsequently mechanically twinned? Irrespective of the origin of the twinned grains, the origin of the untwinned microcline below the temperature of the symmetry transformation seems secure given the absence of a tweed texture indicative of intermediate states of Al–Si order experienced during the cooling of a monoclinic K-feldspar. In the absence of this texture, which is the chief inhibitor to continued ordering of monoclinic K-feldspar during cooling (Brown & Parsons 1989), it is not evident why these grains would not have homogeneously twinned, had they passed through the symmetry break. This again leads to the dilemma of how partially twinned void-filled grains can reflect transformation twinning, if the host grain originates as a triclinic phase.

Discrete precursors to the metasomatic grains have not been identified. It is not evident whether the grains examined formed by solution and precipitation or replacement. If the void-filled grains alone are taken as being metasomatic, only the void-free, twinned grains could be preserved precursors. These twin textures could be consistent with a monoclinic origin, but there remains an absence of supporting evidence, such as textures involving stranded orthoclase. If twinning predated the metasomatism that formed the void-filled grains, the observed textures could simply reflect late-stage replacement of the twinned grains, although again this does not explain the apparent transitions to twinned material seen in many grains. As a general process, replacement of the observed twinned grains by untwinned microcline requires that the least twinned, hence largest grains, be the "youngest" or most altered. This contradicts the relative efficiency of fluid-assisted diffusion processes at grain boundaries and within crystals, where the rate of fluid access to allow dissolution or replacement is proportional to d^{-3} and d^{-2}, respectively, d being the grain diameter. The finest-grained material would be expected to be the most altered, which in this case would require a low density of twins. Instead, with the exception of the late, defect-free grains, the fine-grained matrix exhibits the most homogeneous twin textures. If all grains were primary microcline, dynamic recrystallization would generate the fine-grained matrix, and stress concentrations would be more numerous in the finer grains, where twins are prevalent. If deformation is not related to the twin microstructure, but is imposed later, then the flow stress is significantly greater in the twinned grains, based on the absence of dislocations. Again, a link between the creation of twinned domains and a reduction in dislocation density accommodates this apparent contradiction.

If ore genesis is temporally related to the introduction of the K-feldspar phases we have described, some constraints can be placed on the event. The metasomatism- (voids) and dislocation-related microstructures are not expected to survive the peak conditions of metamorphism and deformation, and are hence assigned to a later stage in the metamorphic history. Although there is rare evidence that these textures developed in feldspar that had been above the temperature of monoclinic ⇌ triclinic transition, the abundance of untwinned, fluid-inclusion-rich triclinic grains favors formation in a lower-temperature, fluid-rich environment. The high degree of average Al–Si order would argue for temperatures lower than the monoclinic ⇌ triclinic transition, although this could simply reflect the efficiency of ordering in the presence of large volumes of fluid, *i.e.*, any evidence of an earlier history would be obliterated. Our current observations define a sequence in which K-feldspar initially occurs as large, untwinned or sparsely twinned grains, which become progressively more homogeneously twinned. There is a concurrent deformation of the untwinned phase and a reduction in grain size, followed by the late-stage introduction or recrystallization of defect-free, untwinned grains. In an evolving system with continued metasomatic activity, the microstructural variations may record a cyclic process of replacement, deformation and recrystallization, of which typically the two most recent generations, linked by transitional grains, are observed. Because such cycles need not be in phase at different localities, even within a thin section, it is not appropriate to assign a discrete event to different portions of the microstructure.

The best indications of an extended history of cooling and metasomatism are the rare examples of tweed texture that contrast with the late-stage, untwinned and undeformed triclinic feldspar. Resolution of whether a progressive variation in grain-scale Al–Si order exists that might support cooling through the transformation temperature could possibly be addressed by detailed application of the ALCHEMI technique, as demonstrated by McLaren & Fitz Gerald (1987). Clearly, there is additional complexity in that we have restricted discussion to the "normal" as opposed to Ba-rich microcline. However, the present observations present new forms of evidence that can contribute to the resolution of these problems.

ACKNOWLEDGEMENTS

LAC Minerals generously supplied the samples and additional support to RLB. NSERC provided financial support through operating grant A8512 to JCW and an infrastructure grant to the UNB Electron Microscopy Unit. Access to the University of Guelph NSERC STEM Facility, with support from T. Beveridge and R. Humphrey, is gratefully acknowledged. Numerous discussions with J. Starkey and comments by R.F. Martin, L.B. Goodwin and A. Park have significantly added to and improved aspects of the paper. D.L. Kohlstedt generously provided facilities to JCW that aided the completion of this work.

REFERENCES

APPLEMAN, D.E. & EVANS, JR., H.T. (1973): Indexing and least squares refinement of powder-diffraction data. *U.S. Geol. Surv., Comput. Contrib.* **20** (NTIS Doc. PB2-16188).

BERTHÉ, D., CHOUKROUNE, P. & JEGOUZO, P. (1979): Orthogneiss, mylonite and non-coaxial deformation of granites: the example of the South Amorican Shear Zone. *J. Struct. Geol.* **1**, 31-42.

BROWN, W.L. (1989a): Glide twinning and pseudotwinning in peristerite: twin morphology and propagation. *Contrib. Mineral. Petrol.* **102**, 306-312.

______ (1989b): Glide twinning and pseudotwinning in peristerite: Si,Al diffusional stabilization and implications for the peristerite solvus. *Contrib. Mineral. Petrol.* **102**, 313-320.

______ & MACAUDIÈRE, J. (1986): Mechanical twinning of plagioclase in a deformed meta-anorthosite – the production of M-twinning. *Contrib. Mineral. Petrol.* **92**, 44-56.

______ & PARSONS, I. (1989): Alkali feldspars: ordering rates, phase transformations and behaviour diagrams for igneous rocks. *Mineral. Mag.* **53**, 25-42.

BURK, R., HODGSON, C.J. & QUARTERMAIN, R.A. (1986): The geological setting of the Teck–Corona Au–Mo–Ba deposit, Hemlo, Ontario, Canada. *In* Proc. Gold '86 Symp. (A.J. Macdonald, ed.), 311-326.

CAMERON, E.M. & HATTORI, K. (1985): The Hemlo gold deposit, Ontario: a geochemical and isotopic study. *Geochim. Cosmochim. Acta* **49**, 2041-2050.

EGGLETON, R.A. & BUSECK, P.R. (1980): The orthoclase–microcline inversion: a high-resolution transmission electron microscope study and strain analysis. *Contrib. Mineral. Petrol.* **74**, 123-133.

FINNEY, J.J. & BAILEY, S.W. (1964): Crystal structure of an authigenic maximum microcline. *Z. Kristallogr.* **119**, 413-436.

FITZ GERALD, J.D. & MCLAREN, A.C. (1982): The microstructures of microcline from some granitic rocks and pegmatites. *Contrib. Mineral. Petrol.* **80**, 219-229.

GANDAIS, M. & WILLAIME, C. (1984): Mechanical properties of feldspars. *In* Feldspars and Feldspathoids (W.L. Brown, ed.). D. Reidel Publishing, Boston (207-246).

GUTHRIE, G.D. & VEBLEN, D.R. (1988): Transmission/analytical electron microscopy of turbid alkali feldspars from the Isle of Skye, Scotland. *Trans. Am. Geophys. Union* **69**, 267 (abstr.).

HARRIS, D.C. (1986): Mineralogy and geochemistry of the main Hemlo gold deposit, Hemlo, Ontario, Canada. *In* Proc. Gold '86 Symp. (A.J. Macdonald, ed.), 297-310.

HUGON, H. (1984): The Hemlo deposits: gold mineralization within a dextral shear zone. *In* Summary of Fieldwork, 1984 (J. Wood, O.L. White, R.B. Barlow & A.C. Colvine, eds.). *Ontario Geol. Surv., Misc. Pap.* **119**, 212-216.

______ (1986): The Hemlo gold deposit, Ontario, Canada: a central portion of a large scale, wide zone of heterogeneous ductile shear. *In* Proc. Gold '86 Symp. (A.J. Macdonald, ed.), 379-387.

KASTNER, M. & SIEVER, R. (1979): Low temperature feldspars in sedimentary rocks. *Am. J. Sci.* **279**, 435-479.

KROLL, H. & RIBBE, P.H. (1987): Determining (Al,Si) distribution and strain in alkali feldspars using lattice parameters and diffraction peak positions: a review. *Am. Mineral.* **72**, 491-506.

KUHNS, R.J., KENNEDY, P., COOPER, P., BROWN, P., MACKIE, B., KUSINS, R. & FRIESEN, R. (1986): Geology and mineralization associated with the Golden Giant deposit, Hemlo, Ontario, Canada. *In* Proc. Gold '86 Symp. (A.J. Macdonald, ed.), 327-354.

LAVES, F. (1952): Mechanische Zwillingsbildung in Feldspäten in Abhängigkeit von Ordnung/Unordnung der Si/Al-Verteilung innerhalb des $(Si,Al)_4O_8$-Gerüstes. *Naturwiss.* **39**, 546-547.

MARSHALL, D.B. & MCLAREN, A.C. (1977): Elastic twinning in experimentally deformed plagioclase feldspars. *Phys. Stat. Sol.* **A41**, 231-240.

MCLAREN, A.C. (1978): Defects and microstructures in feldspars. *In* Chemical Physics of Solids and their Surfaces **7**. The Chemical Society, London (1-30).

______ (1984): Transmission electron microscope investigations of the microstructures of microclines. *In*

Feldspars and Feldspathoids (W.L. Brown, ed.). D. Reidel Publishing, Boston (373-409).

______ & FITZ GERALD, J.D. (1987): CBED and ALCHEMI investigations of local symmetry and Al, Si ordering in K-feldspars. *Phys. Chem. Miner.* **14**, 281-292.

MUIR, T.L. (1983): Geology of the Hemlo - Heron Bay area. *In* The Geology of Gold in Ontario (A. Colvine, ed.). *Ont. Geol. Surv., Misc. Pap.* **110**, 230-239.

______ (1986): Hemlo tectono-stratigraphic study. *In* Summary of Fieldwork, 1986 (P.C. Thurston, O.L. White, R.B. Barlow, M.E. Cherry & A.C. Colvine, eds.). *Ontario Geol. Surv., Misc. Pap.* **132**, 71-74.

______ & ELLIOTT, C.G. (1987): Hemlo tectono-stratigraphic study, District of Thunder Bay. *In* Summary of Fieldwork, 1987 (R.B. Barlow, M.E. Cherry, A.C. Colvine, B.O. Dressler & O.L. White, eds.). *Ontario Geol. Surv., Misc. Pap.* **137**, 117-129.

SMITH, J.V. & BROWN, W.L. (1988): *Feldspar Minerals. 1. Crystal Structures, Physical, Chemical, and Microtextural Properties.* Springer-Verlag, New York.

SMITH, K.L & MCLAREN, A.C. (1983): TEM investigation of a microcline from a nepheline syenite. *Phys. Chem. Miner.* **10**, 69-76.

STARKEY, J. (1964): Glide twinning in the plagioclase feldspars. *In* Deformation Twinning (R.E. Reed-Hill, J.P Hirth & H. Rogers, eds.). *Metall. Soc. Conf.* **25**, 177-191.

______ (1967): On the relationship of Pericline and Albite twinning to the composition and structural state of plagioclase feldspars. *Schweiz. Mineral. Petrogr. Mitt.* **47**, 257-268.

______ & BROWN, W.L. (1964): Küntsliche Erzeugung mechanischer Zwillinge in Anorthit, $CaAl_2Si_2O_8$. *Z. Kristallogr.* **120**, 388-392.

TULLIS, J. (1983): Deformation of feldspars. *In* Feldspar Mineralogy (P.H. Ribbe, ed.). *Rev. Mineral.* **2**, 297-323.

URAI, J.L, SPIERS, C.J., ZWART, H.J. & LISTER, G.S. (1986): Weakening of rock salt by water during long-term creep. *Nature* **324**, 554-557.

VALLIANT, R.I. & BRADBROOK, C.J. (1986): Relationship between stratigraphy, faults and gold deposits, Page–Williams mine, Hemlo, Ontario, Canada. *In* Proc. Gold '86 Symp. (A.J. Macdonald, ed.), 355-361.

VANCE, J.A. (1961): Polysynthetic twinning in plagioclase. *Am. Mineral.* **46**, 1097-1119.

VERNON, R.H. (1965): Plagioclase twins in some mafic gneisses from Broken Hill, Australia. *Mineral. Mag.* **35**, 488-507.

WALFORD, P., STEPHENS, J., SKRECHY, G. & BARNETT, R. (1986): The geology of the "A" zone, Page–Williams mine, Hemlo, Ontario, Canada. *In* Proc. Gold '86 Symp. (A.J. Macdonald, ed.), 362-378.

Received June 22, 1989, revised manuscript accepted April 4, 1990.